

POLARIZATION CANCELLATION IN THE TWO-COMPONENT WINDS FROM WOLF-RAYET STARS

M. TAYLOR

Space Astronomy Laboratory, University of Wisconsin, 1150 University Avenue, Madison, WI 53706

AND

J. P. CASSINELLI

Department of Astronomy, University of Wisconsin, 475 N. Charter Street, Madison, WI 53706

Received 1992 March 9; accepted 1992 June 11

ABSTRACT

It has been suggested that the Wolf-Rayet wind momentum problem can be resolved by assuming that these stars have rotationally enhanced equatorial outflows. The resultant asymmetry of the electron envelope would naturally lead to an intrinsic polarization of the stars. Some, but not all, WR stars are highly polarized. On average, these stars are not as highly polarized as the Be stars, for which there is strong evidence for dense equatorial winds. In addition, the wavelength dependence of the polarization from a WR star in the ultraviolet is different from that expected from an equatorial circumstellar disk of electrons. In this paper we explore the possibility that there can be at least partial cancellation of the equatorial disk polarization as a result of scattering from the electrons that are present in the strong polar wind of WR stars. In order to achieve the cancellation necessary to explain the wavelength-dependent polarization, the polar wind must have a mass-loss rate that is near the maximum that is supported by radiation-driven wind theory. In addition, we find that it is possible to derive important new information regarding the relative column masses of the polar and equatorial winds.

Subject headings: polarization — stars: Wolf-Rayet — stars: mass loss — stars: rotation

1. INTRODUCTION

There is considerable evidence that stellar rotation affects the winds of early-type stars. Although this is particularly evident in the observations of Be stars, similar phenomena are seen in B[e] and Wolf-Rayet (WR) stars as well.

Be stars are rapidly rotating, near-main-sequence B stars which have H α in emission. The *IRAS* satellite found that these stars have strong free-free emission in the infrared. Waters (1986) showed that this excess could originate in a circumstellar equatorial disk, which appears to contain matter that is slowly expanding ($10^{2.5}$ km s $^{-1}$) away from the star (Waters, Coté, & Lamers 1987). Be stars have a low luminosity-to-mass ratio, indicating that the polar wind is much weaker (i.e., with smaller mass-loss rates) than the equatorial wind. Waters et al. (1987) find that the mass-loss rates derived from UV spectroscopic observations are several orders of magnitude lower than those derived from IR excesses. Their interpretation is that the UV lines are sampling the wind in the polar regions of the star while the IR excess arises in the dense equatorial region. In the past few years, several models have been proposed to explain the origin of this strong equatorial outflow. Poe & Friend (1987) first considered the possibility that the disk could be caused by magnetic rotator forces. Pijpers & Hearn (1989) suggested that nonradial pulsations could lead to a dense equatorial outflow. Lamers & Pauldrach (1991) have suggested that a bistability of radiatively driven winds sets in for stars with optically thick Lyman continua; for Be stars this occurs as a result of gravity darkening. More recently, Bjorkman & Cassinelli (1992) developed a two-dimensional model for radiatively driven winds in Be stars. Their model predicts that rapid rotation leads to the formation of high-density material concentrated at low latitudes as a result of shock compression

of the wind in the equatorial plane. As a consequence of enhanced circumstellar material at the equator, Be stars have an intrinsic polarization component which results from electron scattering in the disk. According to Coté & Waters (1987), the continuum polarization is well correlated with the 12 μ m IR excess.

B[e] stars are high-luminosity Be stars (i.e., supergiants) which also exhibit an intrinsic polarization component. Zickgraf et al. (1985) developed an empirical model for the general structure of B[e] stellar winds which is similar to that for Be stars. However, since B[e] stars are more luminous, the mass-loss rate out the poles is larger than that for Be stars. The equatorial or disk winds are also somewhat different, as is evidenced by the IR bumps which indicate the presence of hot (1000 K) dust grains which appear to form in the dense outflowing equatorial material.

In this paper we will concentrate on WR stars and provide evidence about the wind structure of these objects that can be derived from polarization measurements. WR stars eject mass with high terminal velocities (2000 km s $^{-1}$) (Abbott & Conti 1987) and at rates of typically $10^{-5.5} M_{\odot}$ yr $^{-1}$. They have luminosities more comparable to B[e] stars and, even in the absence of rotation, should have strong winds. In particular, the radiation field in the polar regions should drive a wind at least as fast and massive as those from luminous Of stars. This of course is not the case for Be stars which have luminosities that are below the Abbott (1978) limit for strong radiatively driven winds. WR stars are particularly noted for their so-called “wind momentum problem.” The winds of these stars appear to have a substantially larger momentum flux than that which can be explained strictly by radiatively driven wind theory, i.e., if each continuum photon is absorbed or scattered in the circumstellar material so that momentum is transferred

to the wind, then the maximum value for \dot{M} is given by the relation $\dot{M}_{\max} = L/v_{\infty}c$. The maximum mass-loss rate calculated from typical values of L , c , and v_{∞} is an order of magnitude smaller than the mass-loss rate inferred from observations (Schmutz, Hamann, & Wessolowski 1989). This momentum problem has recently been addressed by Cassinelli (1991) and Puls & Pauldrach (1991).

Because of the wind momentum problem, other mechanisms which might act together with radiation pressure to drive the strong, fast, massive winds of WR stars have been proposed. Based on some of the similarities between Be, B[e], and WR stars, Poe, Friend, & Cassinelli (1989, hereafter PFC) suggested that WR stellar winds might be equatorially enhanced. They developed a model which includes effects produced by stellar rotation and corotating magnetic fields. Magnetic and rotational forces can drive a dense equatorial wind which in turn causes the envelope around these stars to be asymmetric. PFC address the momentum problem and argue that the radio observations (Abbott et al. 1986) which are used to determine the stellar mass-loss rates are in fact measuring the denser slower wind material in the equator. As with Be and B[e] stars, the high terminal velocities that are derived from UV line profiles refer to the faster polar wind. Hence, the WR momentum problem is at least in part due to the fact that information concerning two different segments of the wind are combined in deriving the wind momentum, Mv_{∞} .

2. POLARIZATION FROM AXISYMMETRIC DISKS

Brown & McLean (1977) developed equations for the calculation of polarization in early-type stars that have served as the basis for much of the polarization modeling for the past 15 yr. Their model assumes that the central star is a point source which is surrounded by an axisymmetric distribution of scatterers in which the electrons scatter no more than once. Over the past several years, this model has been generalized and some of the limiting assumptions have been lifted. Cassinelli, Nordsieck, & Murison (1987, hereafter CNM) have included a "finite disk correction factor," $D(r)$, which accounts for the angular distribution of the radiation field. At points very close to the stellar surface, the star has a finite size and a single point sees photons which emanate from a wide range of directions. In this case, the net polarization is small. At regions far from the stellar surface, the star appears as a point source, the radiation field is strongly peaked in the forward direction, and the polarization is large. The model was further modified by Brown, Carlaw, & Cassinelli (1989) to account for limb darkening, and recently, polarization effects resulting from occultation of the wind by the star have been calculated by Brown & Fox (1989) and Fox & Brown (1991).

2.1. Observational Properties of WR Stars

A consequence of nonspherically symmetric wind geometries is that the stars should be intrinsically polarized. Based on temporal variability, Moffat (1988) found that only a small fraction of the WR stars in his survey were intrinsically polarized. However, the envelopes of WR stars may be sufficiently stable over short time scales that variability may not be the best indicator of intrinsic polarization. With the development of spectropolarimeters, an alternate method of detecting intrinsic polarization has now become available. If the continuum flux of a WR star is polarized, then the strong emission lines which are formed in the circumstellar material should be depo-

larized, at least to first order. This effect is seen across the H α emission line in Be stars (Poeckert & Marlborough 1978) and in the supergiant P Cygni (Taylor et al. 1991). To date, only four of the 30 WR stars which have been observed spectropolarimetrically have been found to exhibit depolarization across emission lines. From these studies, it is clear that polarimetric observations of WR stars suggest that only a small fraction of these objects are intrinsically polarized. Yet there is adequate reason to believe that these stars may well have equatorially enhanced winds which would lead to a net polarization. Thus arises the central question of this paper: Why are WR stars not as polarized as Be stars?

2.2. Polarization Cancellation Effects in WR Stars

Consider a star that is seen equator-on. Light that is scattered by electrons along the polar axis of the star has its electric vector polarized perpendicular to the polar axis. Light that is scattered by electrons in the equatorial zone has its electric vector polarized parallel to the polar axis. Since the polarization measured by a distant observer is the sum of the polarization produced in the entire region surrounding the star, the net polarization might be smaller than the polarization produced in any one zone. This is what we refer to as the "cancellation effect." In Be stars the polar wind is so much weaker than the equatorial wind that the polarization produced at high latitudes is negligible. This is not the case for WR stars which have much stronger polar winds. In this paper we suggest that WR stars are less polarized than Be stars because there are significant polarization contributions from different parts of the stellar envelope. To determine the extent of this cancellation, we will calculate the polarization produced by electron scattering in the two components of the extended atmosphere of a WR star.

For the WR stars that do show intrinsic polarization, there is another property that might be affected by partial cancellation. This property has to do with the wavelength dependence of the polarization. According to theoretical models for early-type stars, there should be a decrease in polarization across series limits. Be stars, for instance, can show a significant decrease in polarization across the Balmer jump (Bjorkman et al. 1991). This is a result of the fact that when the absorption opacity in the envelope is large, the polarization is small. In the case of WR stars, the polarization has been found to be relatively flat from UV to optical wavelengths (Schulte-Ladbeck et al. 1992).

Hence, there are two polarization cancellation effects that we wish to investigate here: (1) the overall reduction of the continuum intrinsic polarization and (2) the modification of polarization across continuum jumps. Comparison of models with observations will eventually provide useful new information regarding the winds emerging from different sectors of the surface of the star.

3. TWO-COMPONENT WIND MODELS

Our model is similar to that which has been proposed by Zickgraf et al. (1985) for B[e] stars and by Lamers & Waters (1987) for Be stars. As our starting point, we impose one simplification to the PFC model which accounts for the effects of rotation and an open magnetic field. The velocity field in the equatorial plane of a star with a rotationally affected wind has two components, v_r and v_{ϕ} . The azimuthal velocity, v_{ϕ} , increases linearly with r in the solid body rotating region very close to the star and then begins to decrease as $r^{1/2}$ in regions

where there is conservation of gas angular momentum. (The v_ϕ distribution is shown in PFC.) Continuum polarization is expected to be rather insensitive to these details about the azimuthal velocity law, and so, for our present purposes, we have chosen a simpler picture in which there is a radial wind in both the polar and equatorial regions. That is, along the polar angle θ , the density and radial velocity are assumed to be functions of only r .

Our WR star model has two discrete zones: (1) a narrow equatorial zone which has a relatively large mass-loss rate and a comparatively low velocity, and (2) a broad polar zone which has a faster and less dense wind. In the polar region of our two-component wind model, we use the velocity law predicted by radiatively driven wind theory:

$$v(r) = v_0 + v_1 \left(1 - \frac{R_*}{r}\right)^\beta, \quad (1)$$

which has a terminal velocity v_∞ given by the equation $v_\infty^2 = v_0^2 + v_1^2$. We specify v_∞ , and, for simplicity, we assume that the initial velocity, v_0 , is defined to be $0.1v_\infty$. According to CNM, this is a rough approximation to the wind velocity at which there is a significant contrast between the density in and out of the plume. Also, in accordance with a fit to the PFC models, we use $\beta = 0.8$ for the material in the polar zone.

To determine the velocity profile in the equatorial disk, we use the velocity law given in equation (1) with $\beta = 1$ in accordance with the PFC models. Since this material is more optically thick than the polar material, v_0 , is specified as the velocity where $\tau = 1$.

By specifying a mass-loss rate we can calculate the density structure of the extended wind using the conservation of mass:

$$\rho(r) = \frac{\dot{M}}{4\pi r^2 v(r)}. \quad (2)$$

Finally, from specified temperatures of the star and wind, we use the following equation to determine the temperature profile:

$$T(r) = T_* \sqrt{\frac{R_*}{r}}. \quad (3)$$

To calculate the wavelength dependence of the polarization, we need to know the opacity, κ , as a function of frequency and of radial distance. To find this, we use the Sobolev approximation, as was used by CNM for their plume model. At the very least, this approach allows us to account for the basic non-LTE effects that are important in the extended, expanding winds of hot stars. Also, since the densities are different in the polar and equatorial regions, any differences in populations associated with collisional excitation are approximately accounted for.

We realize that the winds of WR stars are sufficiently thick that photons could be scattered more than once as they are transferred through the wind. However, even in WR stars, the single scattering approximation is probably adequate in regard to the production of polarization because there tends to be some neutralization of the polarized light when the photon is scattered a second time. In such a case the net polarization that is observed is that which is produced by the final scattering.

CNM calculated the maximum polarization as a function of wavelength that is produced when mass loss is confined to the polar regions of a star. Here we will apply the same approach

to find the polarization that is produced in a two-component wind. For the special case of equator-on viewing geometry ($\sin i = 1$), the total polarization is given by the equation:

$$P_v = 2 \times [(P_v)_{\text{pole}} + (P_v)_{\text{eq}}], \quad (4)$$

where

$$(P_v)_{\text{pole}} = \frac{3\sigma_T \sin^2 i}{32\pi(1 + \delta_v)} \int_r \int_{\mu=\mu_p}^{\mu=1} n_e(r) e^{-\tau_v(r)} D(r) (1 - 3\mu^2) d\mu dr, \quad (5)$$

$$(P_v)_{\text{eq}} = \frac{3\sigma_T \sin^2 i}{32\pi(1 + \delta_v)} \int_r \int_{\mu=0}^{\mu=1-\mu_p} n_e(r) e^{-\tau_v(r)} D(r) (1 - 3\mu^2) d\mu dr. \quad (6)$$

Here σ_T is the Thomson scattering cross section, i is the inclination angle of the symmetry axis with respect to the observer, δ_v accounts for the added emission produced in the circumstellar environment, $\mu_p = \cos \theta_p$, where θ_p is the half-polar angle, $n_e(r)$ is the electron density in the envelope, $\tau_v(r)$ is the optical depth of the surrounding material, and $D(r)$ is the "finite disk correction factor." In addition to accounting for the finite size of the star, the CNM model also considers the attenuation of continuum photons along the plume which gives rise to a wavelength dependence of the polarization. The opacity, κ_v , is made up of three components: (1) electron scattering opacity which is constant with frequency, (2) bound-free opacity which dominates at short wavelengths, and (3) free-free opacity which becomes important at long wavelengths.

The opening angle of the polar plume is also specified as an input parameter to the model. It is the specification of this angle which defines the limits of the integrands in equations (5) and (6). In the present analysis, we ignore inclination effects and assume an equator-on geometry. We also ignore the emission δ_v from the envelope, as well as the small occultation effects (see Fox & Brown 1991; Fox 1991). According to Fox (1991), for an isothermal wind, occultation of the wind by the star will basically reduce the polarization in the equatorial disk by about 10% and leave the polarization in the plume virtually unchanged. The omission of occultation effects in our models will not modify the results presented in this paper significantly.

4. MODEL RESULTS

We calculate the polarization as a function of wavelength for several different sets of wind parameters; namely, opening angle, mass-loss rates, and velocity law parameters in the polar and equatorial zones. In our first model, we assume the same basic parameters as used by PFC for the WR star, CV Ser. These parameters are based on a two-component wind model assuming a luminosity according to Maeder's mass-luminosity relation (1983). These specified parameters are given in column (2) of Table 1 and the radial dependence of the velocity and density are depicted in Figure 1. In this model, each of the polar zones has an opening angle of 75° , while the half-angle of the equatorial zone is 15° . The polarization results of the PFC model are shown in Figure 2. Very little polarization is produced in the polar wind; the equator is the dominant source of polarization, and, consequently, the "cancellation effect" is small. This is primarily a result of the fact that the bipolar wind flow which was determined by the line-driven wind theory by Friend & Abbott (1986) for O and B stars is small (i.e., a small \dot{M} and a large v_∞ lead to low densities).

TABLE 1
STELLAR WIND PARAMETERS FOR POLARIZATION MODELS

Parameter	PFC Model	Model A
T_{eff}	40,000 K	40,000 K
T_{wind}	30,000 K	30,000 K
v_0 (pole)	340 km s ⁻¹	200 km s ⁻¹
v_0 (equator)	180 km s ⁻¹	180 km s ⁻¹
v_∞ (pole)	3400 km s ⁻¹	2000 km s ⁻¹
v_∞ (equator)	990 km s ⁻¹	990 km s ⁻¹
\dot{M} (pole)	$1.5 \times 10^{-6} M_\odot \text{ yr}^{-1}$	$9.0 \times 10^{-6} M_\odot \text{ yr}^{-1}$
\dot{M} (equator)	$1.1 \times 10^{-5} M_\odot \text{ yr}^{-1}$	$1.1 \times 10^{-5} M_\odot \text{ yr}^{-1}$

Whitney & Code (1992) have made calculations of the polarization as a function of wavelength using the same input parameters as we have used here. Unlike our analytic single-scattering approach, they employ the Monte Carlo method and allow for multiple scattering. Although the Monte Carlo method results in slightly larger polarizations, we find that these two models are in good general agreement and we can assume that our simple approach is good to first order.

Our second model has a slower wind but larger mass-loss rate at the poles than that for the PFC model. The wind

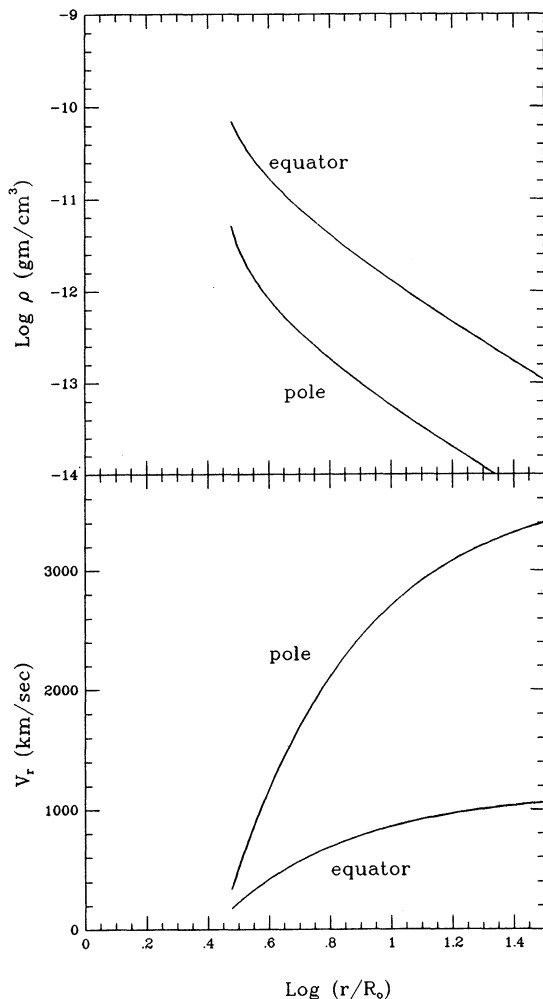


FIG. 1.—Density and velocity as a function of radial distance for the PFC model. The polar wind reaches a terminal velocity of 3400 km s⁻¹, and the equatorial wind reaches a terminal velocity of 990 km s⁻¹.

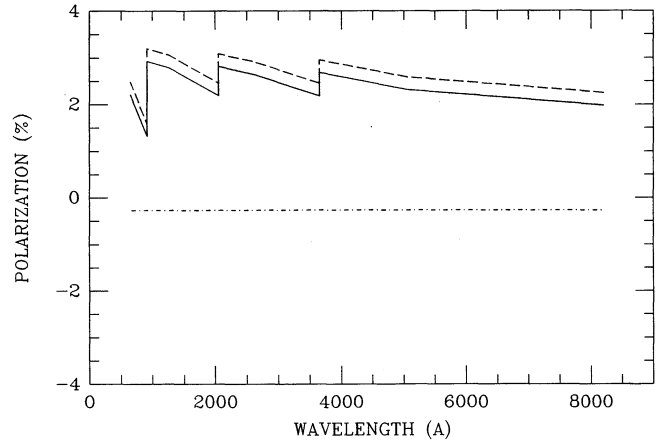


FIG. 2.—The polarization as a function of wavelength for the PFC model. The dashed curve represents the polarization produced in the equatorial disk, the dot-dashed curve represents the polarization produced in the polar plume (note that it is negative), and the solid line denotes the total polarization produced in the entire region of circumstellar material.

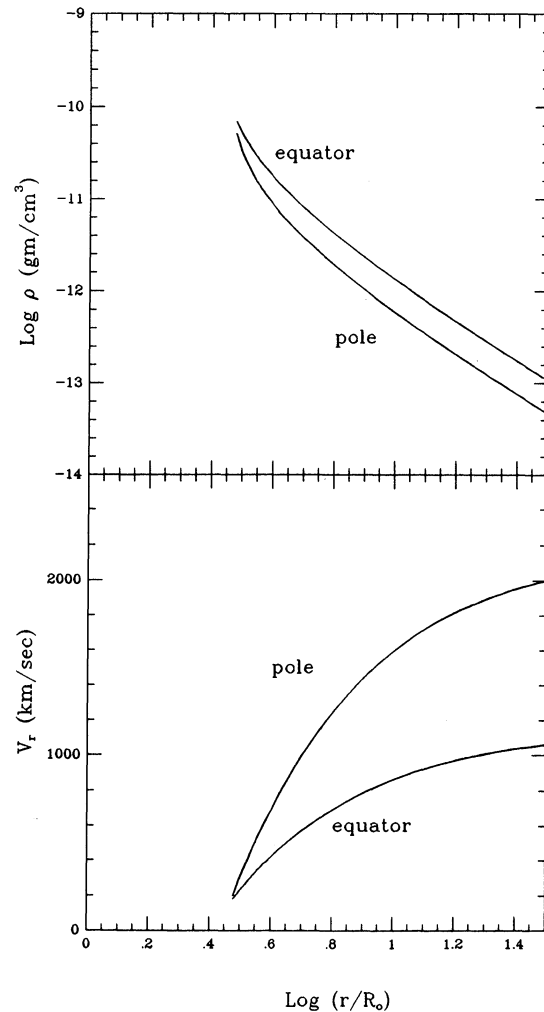


FIG. 3.—Density and velocity as a function of radial distance for the case where the polar wind is driven to its maximum value according to multi-scattering line-driven wind theory called model A. The terminal speed of the polar wind is 2000 km s⁻¹, while that for the equatorial wind remains 990 km s⁻¹.

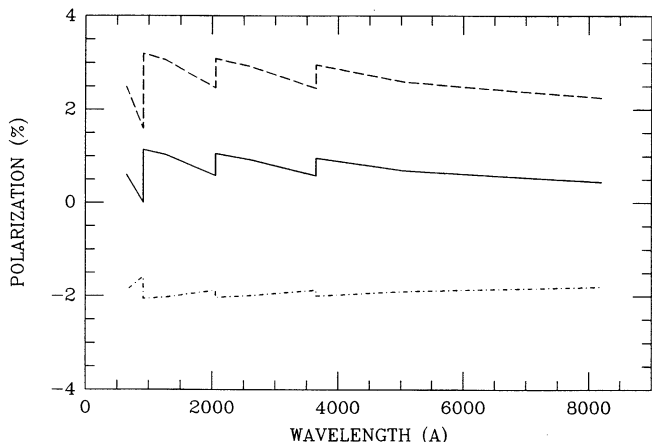


FIG. 4.—The polarization as a function of wavelength for model A in which the polar wind is driven to about the maximum value according to multiscattering line-driven wind theory, $\dot{M} = 9 \times 10^{-6} M_{\odot} \text{ yr}^{-1}$. The notation is the same as that in Fig. 2. Note that the continuum polarization produced in the equatorial disk is reduced by competing polarization in the polar plumes.

parameters for this case are listed in column (3) of Table 1. The velocity and density as a function of radial distance from the star are shown in Figure 3. In this second model, we have driven the mass-loss rate at the poles to about the maximum value according to multiscattering line-driven wind theory.

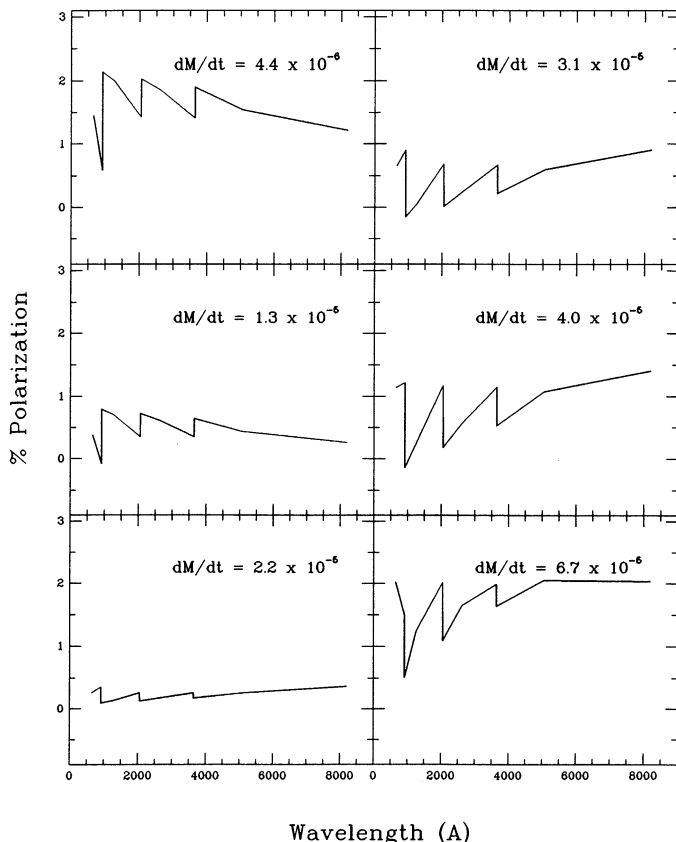


FIG. 5.—The polarization as a function of wavelength for different polar wind mass-loss rates, given in units of $M_{\odot} \text{ yr}^{-1}$. Notice the change in the slope of the Balmer and Paschen continua as well as the change in the amplitude of the polarization across the series limits at 3646 Å, 2050 Å, and 912 Å.

That is, to a value such that the wind momentum is 3 times the stellar radiative momentum. The polarization results of this second model are depicted in Figure 4. We notice that, with the addition of a strong radiatively driven polar wind, there can be significant cancellation of the equatorial wind. Hence, a two-component wind model in which the polar outflow is driven by radiation pressure and an equatorial zone that is driven also by rotation and magnetic forces can lead to significant reduction in the overall continuum polarization of WR stars.

Although previous models in the literature report on decreases in polarization across the series limits, when going to shorter wavelengths, our models suggest a way in which the polarization can show an increase across the limits. In Figure 5 we show a progression of the changes in the polarization curve which results by varying only the polar mass-loss rate. In each of these models all other parameters are exactly those specified in column (3) of Table 1. Notice that the slope of the polarization in the Balmer and Paschen continua gradually change as does the amplitude of the polarization across the hydrogen and helium edges at 3646, 2050, and 912 Å. We find that it is not necessarily the mass-loss rate which gives rise to these changes in polarization, but, rather, the ratio \dot{M}/v_{∞} . To show this, we computed several models. We found that if one varied \dot{M}_p and $v_{\infty,p}$ in such a way that the ratio $(\dot{M}/v_{\infty})_p$ was held constant, there was essentially no change in the polarization curve. However, if the ratio $(\dot{M}/v_{\infty})_p/(\dot{M}/v_{\infty})_{\text{eq}}$ varied, there were significant changes in the wavelength dependence of the polarization. Figure 6a shows the change in slope of the Balmer continuum, defined between 2052 Å and 3646 Å, and Figure 6b shows the corresponding variation in the amplitude of the change in polarization across the Balmer edge. Models for both a $\beta = 1$ and a $\beta = 0.8$ polar velocity law were calculated, but the only difference was a slight horizontal shift in the resulting curves. It is immediately obvious from Figure 6 that when the slope in the continuum is negative, the polarization decreases across the Balmer jump and when the slope is positive, the polarization increases across the series limit. The same behavior prevails in the other edges at 2050 Å and 912 Å as well. Notice that as the polar wind becomes stronger, the slope of the Balmer continuum becomes less negative and the Balmer discontinuity becomes weaker. The slope of the polarization curve reaches zero and the Balmer jump vanishes when $(\dot{M}/v_{\infty})_p d\Omega = (\dot{M}/v_{\infty})_{\text{eq}} d\Omega$. A continued increase in the polar wind results in an increase in the steepness of the polarization curve and a decrease in the size of the depolarization across the Balmer edge. Eventually, the optical depth in the polar plume becomes so large (and hence, $e^{-\tau}$ becomes small) that the polarization produced in the polar wind becomes negligible; the equatorial wind again begins to dominate and both curves asymptotically approach a maximum or minimum value. Figure 6 suggests that the wavelength dependence of the polarization may be an important tool for determining the relative column masses of polar and equatorial winds.

Recently, Taylor et al. (1991) presented spectropolarimetric observations of the hypergiant P Cygni. Their data indicate that the polarization can either increase or decrease at the hydrogen Balmer discontinuity, depending on the temporal state of the wind. Taylor et al. (1991) suggest that P Cyg ejects blobs or shells of material intermittently and in random directions. Given the rotation of position angle with wavelength, they suggest that multiple regions of density-enhanced material may persist in the circumstellar environment of P Cyg at any given time. One might be able to explain the polari-

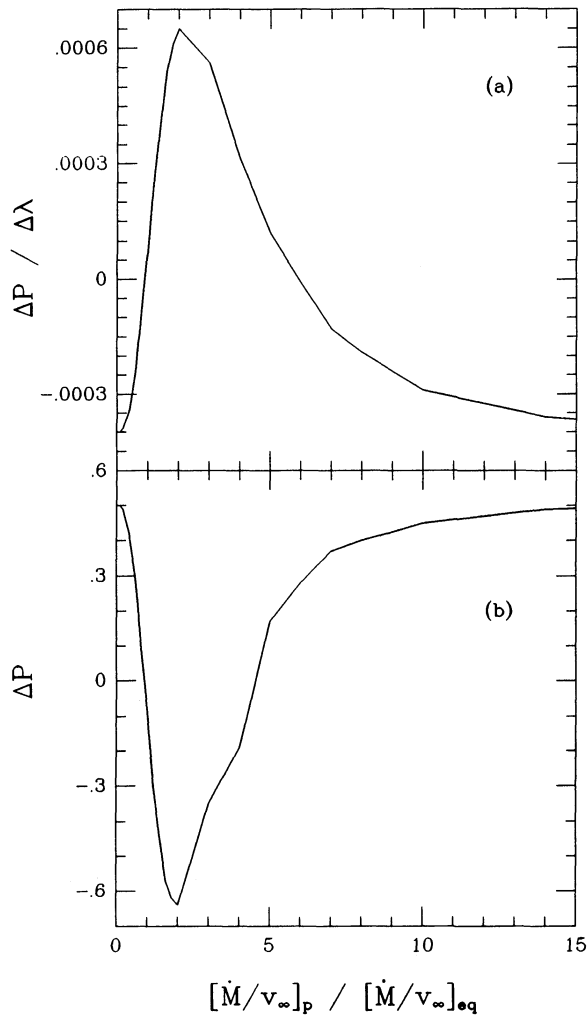


FIG. 6.—The top curve is a depiction on the variation of the slope on the Balmer continuum (see text) with increasing $(\dot{M}/v_\infty)_p/(\dot{M}/v_\infty)_{eq}$ and the bottom figure is a similar plot of the change in polarization across the Balmer edge.

metry of P Cyg by assuming that when the polarization increases at 3646 Å, the material in the polar zone of the star is more dominant. When the polarization decreases at the Balmer jump, density-enhanced material in the equatorial region of the star dominates over material in the polar zone.

5. CONCLUSIONS

In this paper, we have calculated the polarization produced in a two-component wind in order to explain why WR stars have polarizations which are generally lower than those for Be stars. In addition, our results lend support for the idea that WR stars have rotationally enhanced equatorial outflows. Our two-component wind model consists of a broad polar plume which is driven strictly by radiation pressure and a narrow equatorial disk whose characteristic properties are determined by the addition of rotation and magnetic forces. Our models show that when there are regions of the circumstellar material which have distinctly different wind parameters, there is a competition between the polarization produced in the various zones. In our specific case of a slow but dense equatorial wind accompanied by a fast but more tenuous polar wind, we find that the polarization produced in the polar zone can significantly cancel the polarization produced in the more optically thick material at the equator. This is simply a result of the fact that the direction of the polarization produced in the polar material is exactly perpendicular (and hence, negative) to the direction of the polarization produced in the disk. In addition to this overall reduction of the continuum polarization, we show that the wavelength dependence of the polarization produced in the two-component wind model can differ from that previously reported in the literature for other geometries. The basic idea is that if the polarization produced in the poles dominated over that produced in the disk, then, rather than decreasing across the series limits, the total polarization increases. This is accompanied by a corresponding change in the slope of the Balmer and Paschen continua.

We would like to thank Arthur Code and Barbara Whitney for numerous discussions and model comparisons. Thanks also to Geoffrey Fox for offering useful suggestions to this paper. This research has been supported by NASA contract NAS5-26777 and NAGW422.

REFERENCES

- Abbott, D. C. 1978, *ApJ*, 225, 893
 Abbott, D. C., Biegging, J. H., Churchwell, E., & Torres, A. V. 1986, *ApJ*, 303, 239
 Abbott, D. C., & Conti, P. S. 1987, *ARA&A*, 25, 113
 Bjorkman, J., & Cassinelli, J. P. 1992, *ApJ*, submitted
 Bjorkman, K. S., et al. 1991, *ApJ*, 383, L67
 Brown, J. C., Carlaw, V. A., & Cassinelli, J. P. 1989, *ApJ*, 344, 341
 Brown, J. C., & Fox, G. K. 1989, *ApJ*, 347, 468
 Brown, J. C., & McLean, I. S. 1977, *A&A*, 57, 141
 Cassinelli, J. P. 1991, in *Wolf-Rayet Stars and Interrelations with Other Massive Stars in Galaxies*, ed. K. A. van der Hucht & B. Hidayat (Dordrecht: Kluwer), 289
 Cassinelli, J. P., Nordsieck, K. H., & Murison, M. A. 1987, *ApJ*, 317, 290 (CNM)
 Coté, J., & Waters, L. B. F. M. 1987, *A&A*, 176, 93
 Fox, G. K. 1991, *ApJ*, 379, 663
 Fox, G. K., & Brown, J. C. 1991, *ApJ*, 375, 300
 Friend, D. B., & Abbott, D. C. 1986, *ApJ*, 311, 701
 Lamers, H. J. G. L. M., & Pauldrach, A. W. A. 1991, *A&A*, 244, L5
 Lamers, H. J. G. L. M., & Waters, L. B. F. M. 1987, *A&A*, 182, 80
 Maeder, A. 1983, *A&A*, 92, 101
 Moffat, A. F. J. 1988, in *Polarized Radiation of Circumstellar Origin*, ed. G. V. Coyne, S. J., et al. (Vatican: Vatican Observatory), 603
 Pijpers, F. P., & Hearn, A. G. 1989, *A&A*, 209, 198
 Poe, C. H., & Friend, D. B. 1987, in *IAU Colloq. 92*, ed. A. Slettebak & T. P. Snow (Cambridge: Cambridge Univ. Press), 437
 Poe, C. H., Friend, D. B., & Cassinelli, J. P. 1989, *ApJ*, 337, 888 (PFC)
 Poeckert, R., & Marlborough, J. M. 1978, *ApJ*, 220, 940
 Puls, J., & Pauldrach, A. W. A. 1991, in *Stellar Atmospheres: Beyond Classical Models* (Dordrecht: Reidel)
 Schmutz, W., Hamann, W.-R., & Wessolowski, U. 1989, *A&A*, 210, 236
 Schulte-Ladbeck, R. E., et al. 1992, *ApJ*, 391, L37
 Taylor, M., Nordsieck, K. H., Schulte-Ladbeck, R. E., & Bjorkman, K. S. 1991, *AJ*, 102, 1197
 Waters, L. B. F. M. 1986, *A&A*, 162, 121
 Waters, L. B. F. M., Coté, J., & Lamers, H. J. G. L. M. 1987, *A&A*, 185, 206
 Whitney, B. A., & Code, A. D. 1992, in preparation
 Zickgraf, F.-J., Wolf, B., Stahl, O., Leitherer, C., & Klare, G. 1985, *A&A*, 143, 421